

# Conditional loss of the exocyst component Exoc5 in retinal pigment epithelium (RPE) results in RPE dysfunction, photoreceptor cell degeneration, and decreased visual function.

Bärbel Rohrer<sup>1,2#</sup>, Elisabeth Obert<sup>1</sup>, Yujing Dang<sup>3</sup>, Yanhui Su<sup>3</sup>, Xiaofeng Zuo<sup>3</sup>, Ben Fogelgren<sup>4</sup>, Manas R. Biswal<sup>5</sup>, Altaf A. Kondkar<sup>6</sup>, Glenn P. Lobo<sup>1,3,7\*#</sup> and Joshua H. Lipschutz<sup>1,8#</sup>

<sup>1</sup>Department of Ophthalmology, Medical University of South Carolina, Charleston, SC, 29425, USA.

<sup>2</sup>Ralph H. Johnson VA Medical Center, Division of Research, Charleston, SC 29401.

<sup>3</sup>Department of Medicine, Medical University of South Carolina, Charleston, SC, 29425, USA. <sup>4</sup>

Department of Anatomy, Biochemistry, and Physiology, University of Hawaii at Manoa, Honolulu, HI 96813, USA.

<sup>5</sup>Department of Pharmaceutical Sciences, Taneja College of Pharmacy, University of South Florida, Tampa, FL 33612, USA.

<sup>6</sup>Department of Ophthalmology, College of Medicine, King Saud University, Riyadh 11411, Saudi Arabia.

<sup>7</sup>Department of Ophthalmology and Visual Neurosciences. Lions Research Building, 2001 6th Street SE., Room 225, University of Minnesota, Minneapolis, MN 55455, USA.

<sup>8</sup>Department of Medicine, Ralph H. Johnson Veterans Affairs Medical Center, Charleston SC, 29425, USA.

**\*Corresponding Author:** Glenn P. Lobo, Ph.D., Associate Professor, Department of Ophthalmology and Visual Neurosciences, Lions Research Building, 2001 6th Street SE., Room LRB 225 University of Minnesota Minneapolis, MN 55455, USA. E-mail: [lobo0023@umn.edu](mailto:lobo0023@umn.edu).

# equally supervised this work

**Abstract:** To characterize the mechanisms by which the highly-conserved exocyst trafficking complex regulates eye physiology in zebrafish and mice, we focused on exoc5 (aka *sec10*), a central exocyst component. We analyzed both *exoc5* zebrafish mutants and retinal pigmented epithelium (RPE)-specific *Exoc5* knockout mice. Exoc5 is present in both the non-pigmented epithelium of the ciliary body and in the RPE. In this study we set out to establish an animal model to study the mechanisms underlying the ocular phenotype and to establish if loss of visual function is induced by postnatal RPE Exoc5-deficiency. *Exoc5*<sup>-/-</sup> zebrafish showed smaller eyes, with decreased number of melanocytes in the RPE and shorter photoreceptor outer segments. At 3.5 days post fertilization, loss of rod and cone opsins were observed in zebrafish Tg:*exoc5* mutants. Mice with postnatal RPE-specific loss of Exoc5 showed retinal thinning associated with compromised visual function, and loss of visual photoreceptor pigments. This retinal

phenotype in *Exoc5*<sup>-/-</sup> mice was present at 20-weeks, and the phenotype was more severe at 27-weeks, indicating progressive disease phenotype. We previously showed that the exocyst is necessary for photoreceptor ciliogenesis and retinal development. Here, we report that *exoc5* mutant zebrafish and mice with RPE-specific genetic ablation of *Exoc5* develop abnormal RPE pigmentation, resulting in retinal cell dystrophy and loss of visual pigments associated with compromised vision. As RPE cells are “downstream” of photoreceptor cells in the visual process, these data suggest exocyst-mediated retrograde communication and dependence between the RPE and photoreceptors.

**Keywords:** retinal pigmented epithelium, exocyst complex component 5, photoreceptor, visual function.

---

## 1. Introduction

In developed countries, such as the U.S., glaucoma and cataracts are treated relatively easily, so the most common cause of blindness is, or soon will be, retinal degenerative diseases [1]. Already, retinal diseases are the most common cause of childhood blindness worldwide [2]. In turn, almost one-quarter of known retinal degeneration genes in the Retinal Information Network (RetNet) are associated with ciliary function and intracellular trafficking [3]. Cilia, found on the surface of many eukaryotic cell types, are thin rod-like organelles extending outward from the basal body, a cellular organelle related to the centriole. Cilia are classified as primary (non-motile) or motile and contain a central axoneme composed of microtubules. In epithelia containing numerous motile cilia, cilia have a propulsive function, while primary cilia have a mechano- and chemosensory function [4]. It has been known for over 100 years that epithelial cells possess primary cilia; however, little had been ascribed regarding function, and primary cilia had even been considered to be vestigial [5]. Over the past decade, cilia have been shown to be central to the pathogenesis of “ciliopathies” that affect many organs, including the kidney and eye. We discovered that the exocyst a highly conserved eight-protein trafficking complex and its regulators are necessary for cilia formation in kidney and eye cells<sup>1,4-7,9</sup>. In a series of studies, we elucidated the critical role that the highly conserved eight-protein exocyst trafficking complex plays in retinal and renal ciliogenesis[6-10].

Exocyst Complex Component 5 (*Exoc5*; also known as *Sec10*) is a central component of the exocyst complex [11]. The defect in eye development that we identified following antisense morpholino knockdown of *exoc5* in zebrafish, originally performed to study the role of the exocyst in renal ciliogenesis/development, was a serendipitous finding [12]. During the course of these studies we noticed small eyes in morphant zebrafish, and went on to demonstrate severe defects in cilia/eye development, following antisense morpholino knockdown of *exoc5* and the small GTPase *cdc42*, a regulator of the exocyst

[12]. This led us to hypothesize that exocyst-mediated ciliogenic programs are conserved across organs and species, and that the exocyst is centrally involved in mammalian eye development.

In the eye, photoreceptor and retinal pigmented epithelial (RPE) cells are ciliated. Mutations in exocyst proteins cause Joubert Syndrome [13], a ciliopathy associated with kidney and retinal phenotypes [14]. Our recently published data show two *exoc5* mutant zebrafish lines phenocopying *exoc5* morphants, with grossly abnormal photoreceptor and RPE cells [15]. Using our *Exoc5* floxed mice [16], and *Rhodopsin-Cre* mice, we generated *Exoc5* photoreceptor-specific knockout (KO) mice that, strikingly, showed progressive loss of photoreceptor cells and, by six weeks of age, were devoid of any visual response [15]. Overall, these data showed that exocyst-mediated ciliogenesis is conserved across species and organs. The progressive loss of the photoreceptor outer segments, which are modified primary cilia, in our zebrafish and mouse models was striking, and led to blindness.

Given our previous results showing *Exoc5* is necessary for ciliogenesis in photoreceptor cells in zebrafish and mice [15], and that *cdc42* and *exoc5* are necessary for retinal development in zebrafish and interact synergistically [12], in this study we investigated the role of *Exoc5* in RPE cell ciliogenesis and retinal development using RPE-specific *Bestrophin1-Cre* (*Best1-Cre/+*) mice [17]. Somewhat surprisingly, as RPE cells are “downstream” of photoreceptor cells in the visual process, we found RPE-specific knockout of *Exoc5* led to retinal cell dystrophy and loss of visual pigments in photoreceptors and was associated with compromised vision.

## 2. Results

### 2.1. Loss of *exoc5* in zebrafish results in RPE and photoreceptor phenotypes

We obtained *exoc5*<sup>-/-</sup> zebrafish lines (from the Zebrafish International Resource Consortium (ZIRC), # *exoc5* sa23168). At 3.5 days post fertilization (dpf) we observed that all *exoc5*<sup>-/-</sup> mutants had smaller eyes when compared to wild-type (WT) siblings [15]. The eye morphologic phenotype was consistently observed in ~25% of the progeny from crosses of heterozygous parents as would be expected for Mendelian inheritance of a recessive mutation. Detailed histological examination and H&E staining of 3.5 dpf *exoc5*<sup>-/-</sup> retinas showed thinning of the retinal pigmented epithelium (RPE) and photoreceptor layers (**Fig.1A**). By transmission electron microscopy (TEM) we confirmed shorter photoreceptor outer segments (OS), hypopigmentation, and fewer melanosomes in *exoc5*<sup>-/-</sup> retinas (**Figs. 1B and 1C**). Such abnormalities were never observed in retinal sections of WT siblings. Taken together, these results indicate that eye development, proper retinal lamination, RPE health, and outer segment morphogenesis requires *Exoc5* function in zebrafish.

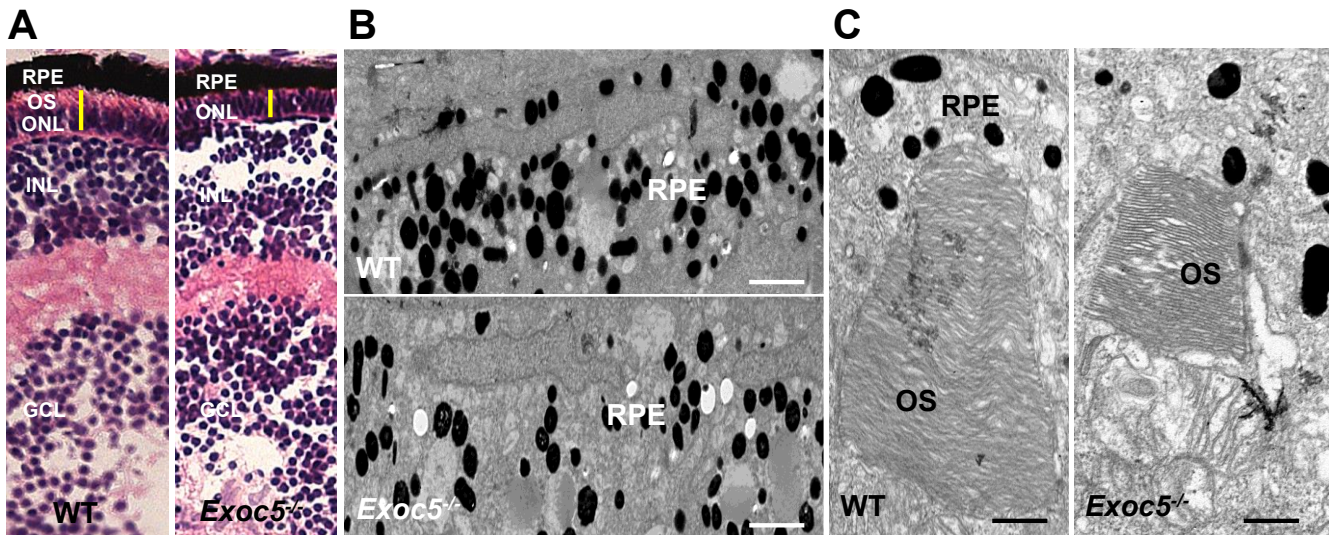


**Fig. 1. Histological and TEM analysis of RPE and retinas of wild-type and *exoc5* mutant zebrafish larvae.**

(A) In *exoc5* homozygous mutants the photoreceptor outer segments (OS) were shorter, compared to wild-type (WT) siblings. (B) Ultrastructural analysis of WT and *exoc5* mutant RPE and photoreceptors using transmission electron microscopy. (C) WT photoreceptors showed tightly stacked disc membranes, while in *exoc5* mutants only remnants of outer segments (OS) could be observed. Scale bars=2  $\mu$ m (B), 800 nm (C). OS, outer segments; ONL, outer nuclear layer; RPE, Retinal Pigmented Epithelium; INL, Inner Nuclear Layer; Ganglion Cell Layer, GCL.

## 2.2. Loss of *Exoc5* in zebrafish results in early retinal phenotypes

We next performed a detailed immunohistochemical analysis in *exoc5*<sup>-/-</sup> zebrafish to determine if localization and trafficking of photoreceptor outer segment proteins occurred normally in *exoc5* mutants. At 3.5 dpf, ZPR3 localized normally to the rod outer segments of WT zebrafish (Fig. 2A). In *exoc5* mutants, rudimentary outer segment localization of ZPR3

was observed (**Fig. 2A**). To quantify the lengths of the outer segments, we used ZPR3 immunoreactivity as a surrogate, determining the extent of ZPR3 staining along the proximal-distal axis of the outer segments. In WT siblings, outer segments were  $6.88 \pm 0.28 \mu\text{m}$  in length ( $n=25$  embryos, 300 outer segments), while *exoc5* mutant outer segments were  $2.56 \pm 0.12 \mu\text{m}$  in length ( $P < 0.001$ ;  $n=18$  embryos, 200 outer segments) (**Fig. S2**). We then examined cone morphology, the predominant photoreceptor cell type in the zebrafish retina, by immunolabeling with peanut agglutinin lectin (PNA-488), which labels the interphotoreceptor matrix surrounding cone outer segments, and, to some extent, the retinal plexiform layers (19). PNA-488 staining revealed that the *exoc5* mutant cone outer segments were significantly shorter ( $5.65 \pm 0.30 \mu\text{m}$  in WT vs.  $2.96 \pm 0.25 \mu\text{m}$  in mutants;  $P < 0.001$ ), disorganized and misshapen (**Fig. 2B and Fig. S2**). Additionally, immunohistological staining using R/G cone opsin antibody, we observed that the number of cone outer segments were significantly fewer in number and shorter in *exoc5* mutants compared to WT siblings (**Fig. 2C**), which suggested that loss of *exoc5* results in defective cone outer segment morphogenesis. Heterozygous *exoc5*<sup>+/-</sup> mutant carriers were then outcrossed for 2 generations with WT-Tg:XOPS-GFP [*Tg(XIRho:EGFP)<sup>fl1</sup>*], zebrafish line, which expresses soluble GFP under the control of Rhodopsin in rod photoreceptor cells only [20]. The F3 generation heterozygous *exoc5* mutant carriers (*exoc5*<sup>+/-</sup>;Tg:XOPS-GFP) were crossed and retinas stained with R/G cone opsins. This analysis further confirmed endogenous loss of Rhodopsin protein in rods, and loss of cone opsins in retinas of *exoc5*<sup>-/-</sup>;Tg:XOPS-GFP mutants (**Fig. 3**) These data demonstrate that *exoc5* is indispensable for photoreceptor outer segment formation and maintenance in zebrafish. Because *exoc5*<sup>-/-</sup> zebrafish represented a global knockout of *exoc5*, we did not know if the loss of *exoc5* in photoreceptors and/or the RPE led to the phenotype. To dissect out a mechanism, we generated a mouse model.

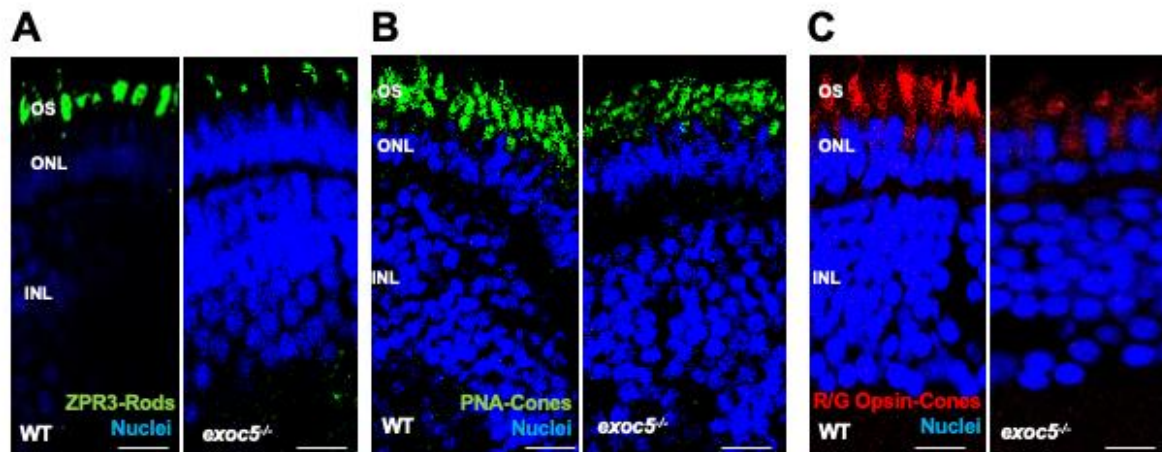


**Fig. 2. Immunohistochemical analysis of rod and cone photoreceptors in wild-type and *exoc5*<sup>-/-</sup> mutant zebrafish.** Rod photoreceptor outer segments were identified with ZPR3 antibody (green, ZPR3, **A**), cone photoreceptors with PNA-lectin-488 (green, PNA, **B**), and medium-wavelength R/G cone opsins (red, R/G Opsin, **C**), all at 3.5 dpf. Severe loss of rod and cone OS was noted in *exoc5*<sup>-/-</sup> mutant zebrafish. Scale bars= 50 μm (**B**) and 25 μm (**A**, **C**). OS, outer segments; ONL, outer nuclear layer; INL, Inner Nuclear Layer.

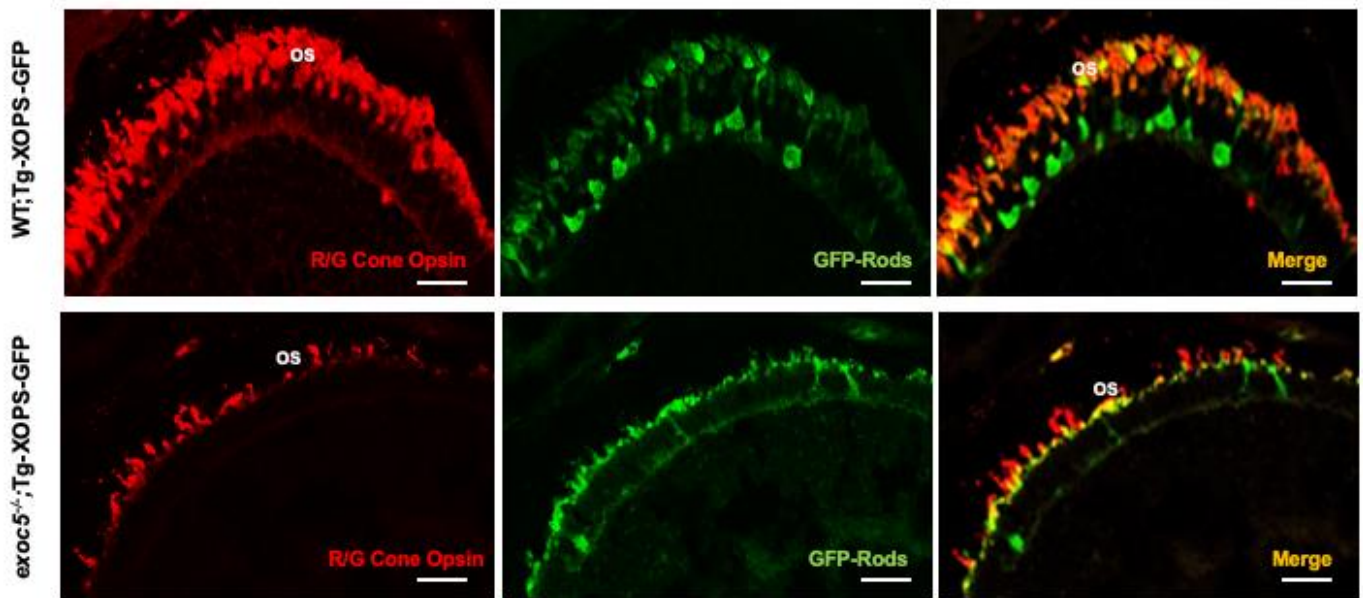


**Fig. 3: Immunohistochemical analysis of rod and cone photoreceptors in transgenic (Tg:XOPS) wild-type and *exoc5* mutant zebrafish.** Top Panel: Wild-type:Transgenic-XOPS (WT;Tg-XOPS-GFP) zebrafish retinas immunostained with R/G cone opsin (red). Bottom Panel: *exoc5*<sup>-/-</sup> mutant:Transgenic-XOPS (*exoc5*<sup>-/-</sup>;Tg-XOPS-GFP) retinas immunostained with R/G cone opsin (red). The transgenic line expresses soluble endogenous GFP in rods (green). Significantly shorter rod and cone OS were observed in *exoc5*<sup>-/-</sup> mutant zebrafish, compared to WT zebrafish, at similar ages.

### 2.3. RPE-Specific Ablation of Exoc5 in mice cause retinal cell degeneration

Both retinal pigmented epithelium (RPE) and photoreceptor cells are normally postmitotic in the healthy adult mammalian eye. Thus, interactions between specific photoreceptor outer segments (OS) and RPE cells persist for life. Importantly, as RPE cells

cover much larger areas of the retina than individual photoreceptor cells, each RPE cell faces between 30 and 50 photoreceptor OS. Depending on its location in the retina, an individual RPE cell faces and functionally interacts with cones, rods, or (in most cases) a mixture of the two. To determine the role of EXOC5 in RPE for photoreceptor health in a mammalian model, Ai14 Cre reporter mice that harbor a *loxP*-flanked STOP cassette preventing transcription of a CAG promoter-driven red fluorescent protein variant (*tdTomato*), congenic on the C57BL/6J genetic background, were mated to *Exoc5<sup>fl/fl</sup>* mice, so that *tdTomato* expression in a cell indicates that *Exoc5* has been inactivated by Cre. To investigate the physiologic role of EXOC5 in the retina we produced mice with RPE-selective loss of EXOC5 in the early postnatal period by crossing mice bearing floxed *Exoc5* alleles (*tdTomatoExoc5<sup>lox/fllox</sup>*) with mice transgenic for *BEST1-Cre*. Deletion of *Exoc5* in RPE cells was confirmed by *tdTomato* expression (red color) in RPE cells of *tdTomatoExoc5<sup>fl/fl</sup>;Best1-Cre/+*, compared to *tdTomatoExoc5<sup>fl/fl</sup>* mice (**Fig. S1**). We analyzed retinas of mice at 20- and 27-weeks of age. Here, retinal histology of *Exoc5<sup>fl/fl</sup>;Best1-Cre/+* mice at 20-weeks of age showed normal morphology with slightly thinner photoreceptor outer segments (OS), when compared to controls (**Figs. 4A and 4A'**). Transmission electron microscopy (TEM) analysis confirmed that OS in *Exoc5<sup>fl/fl</sup>;Best1-Cre/+* mutants were ~16-20% shorter than those in age-matched littermate controls ( $P<0.05$ ). *Exoc5<sup>fl/fl</sup>;Best1-Cre/+* mice at 27-weeks of age showed thinner outer nuclear layer (ONL), and even shorter photoreceptor OS, when compared to controls (*tdTomatoExoc5<sup>fl/fl</sup>*) mice (**Figs. 5A and 5B**). Disorganization and shorter photoreceptor outer segments (~82-87% shorter than controls;  $P<0.005$ ) was more obvious by transmission electron microscopy of conditional *Exoc5* knockout animals (**Figs. 5C and 5C'**). These data show the importance of EXOC5 expression in RPE cells for retinal cell maintenance. The more severe effect at 27 weeks was likely due to the fact that maximum cre expression in the *Best1-Cre* mouse occurs at P28 [17].

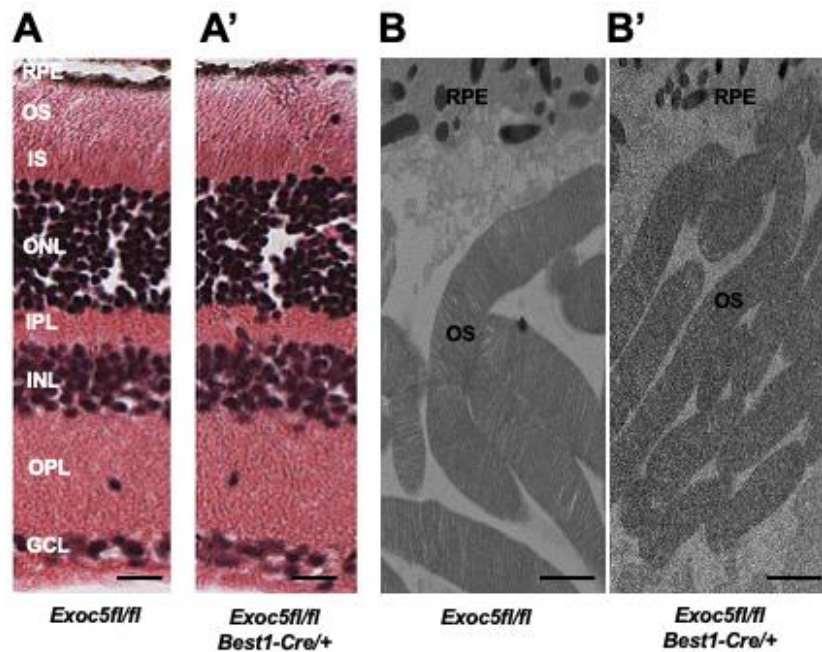


**Fig. 4.** Histological and TEM analysis of retinas of *Exoc5<sup>-/-</sup>* mutants and *WT* mice at 20-weeks of age. (A, A') H&E staining of WT and *Exoc5<sup>-/-</sup>* retinas at 20-weeks. (B, B') Transmission electron microscopy provided ultrastructural views of wild-type (WT) mice photoreceptor cells. Scale bars= 800 nm. RPE, Retinal pigmented epithelium; PRL, photoreceptor cell layer; ONL, outer nuclear layer; INL, Inner Nuclear Layer.

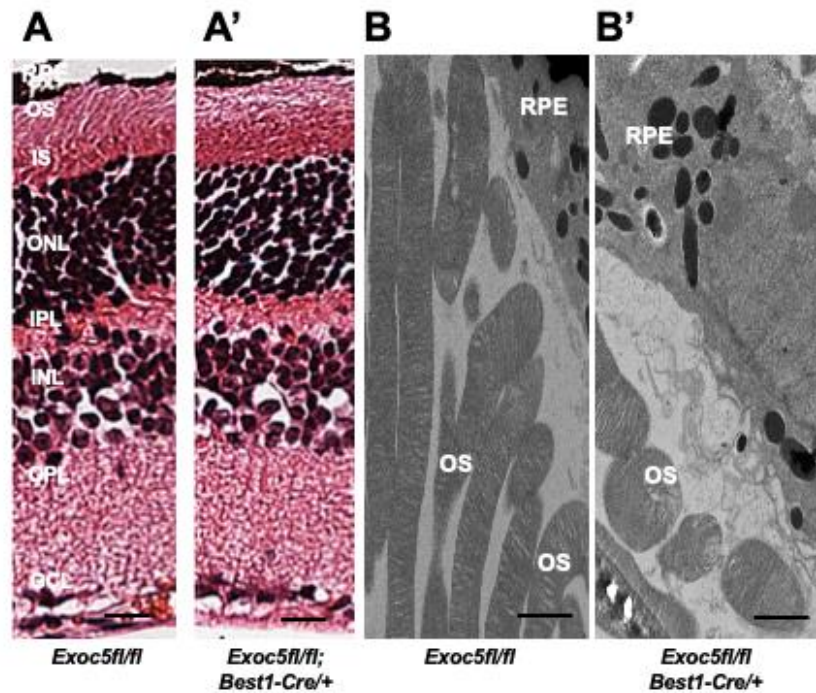


**Fig. 5.** Histological and TEM analysis of retinas of *Exoc5*<sup>-/-</sup> mutants and WT mice at 27-weeks of age. (A, A') H&E staining of WT and *Exoc5*<sup>-/-</sup> retinas at 27-weeks. (B, B') Transmission electron microscopy of WT and *Exoc5*<sup>-/-</sup> photoreceptor cells. Scale bars= 800 nm (B, B'). RPE, Retinal pigmented epithelium; PRL, photoreceptor cell layer; ONL, outer nuclear layer; INL, Inner Nuclear Layer.

#### 2.4. Conditional *Exoc5* knockout mice show defects in photoreceptor development

To determine if localization and trafficking of photoreceptor outer segment proteins occurred normally in *Exoc5<sup>fl/fl</sup>;Best1-Cre<sup>+</sup>* mice, we performed a detailed immunohistochemical for RPE proteins and photoreceptor opsins. In both WT and *Exoc5<sup>fl/fl</sup>;Best1-Cre<sup>+</sup>* mice, rhodopsin was localized to the outer segments by 20-weeks of age, however rhodopsin staining in *Exoc5<sup>fl/fl</sup>;Best1-Cre<sup>+</sup>* mice was moderately reduced (**Fig. 6A and Fig. S2**). *Exoc5<sup>fl/fl</sup>;Best1-Cre<sup>+</sup>* mouse retinas at 27-weeks of age exhibited significantly decreased levels of rhodopsin (**Fig.7A and Fig. S2**). As we did for zebrafish retinas, rhodopsin immunoreactivity along the axis of the outer segment was used to document a shortened outer segment length in mutant mice (**Fig. S2**). Cone morphology was examined by immunolabeling with anti-Red/Green cone opsin antibody. Cone opsin staining revealed the presence of long and well-organized cone outer segments in WT mice at 20-weeks, whereas *Exoc5<sup>fl/fl</sup>;Rho-Cre<sup>+</sup>* mouse cone outer segments at 27-weeks were significantly shorter and appeared disorganized and misshapen (**Figs. 6B, 7B and Fig. S2**). Finally, integrity of the retinal pigmented epithelium was accessed using RPE65 staining. This analysis showed a progressive decrease in RPE65 protein in retinas of *Exoc5<sup>fl/fl</sup>;Best1-Cre<sup>+</sup>* mice (**Figs. 6C and 7C**). These results demonstrate that loss of *exoc5* in the RPE is crucial for cilia and rod photoreceptor outer segment formation in mice.

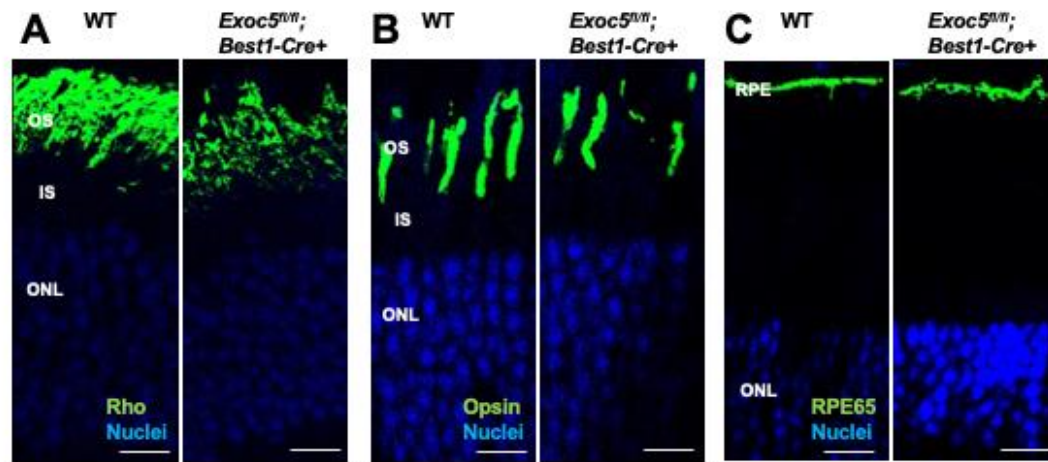
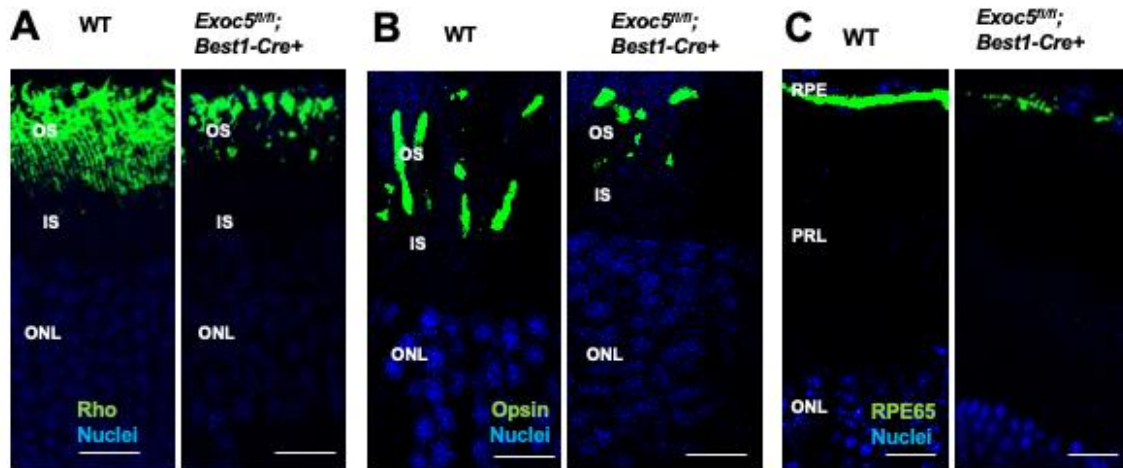


Fig. 6.

Immunohistochemical analysis of rod and cone photoreceptors in wild-type and conditional *Exoc5* knockout mice at 20-weeks of age.

(A) Levels and localization of rhodopsin (green, Rho, A), cone photoreceptors with R/G cone opsins (green, Opsin R/G, B), and retinal pigmented epithelium with RPE65 (green, RPE65, C), were used at 20-weeks of age to identify alterations in in rod and cone outer segments. Scale bars= 50 μm (A, B, and C). OS, outer segments; IS, inner segments; ONL, outer nuclear layer, INL, inner nuclear layer; RPE, retinal pigmented epithelium.



**Fig. 7. Immunohistochemical analysis of rod and cone photoreceptors in wild-type and conditional *Exoc5* knockout mice at 27-weeks of age.**

(A) Levels and localization of rhodopsin (green, Rho, A), cone photoreceptors with R/G cone opsins (green, Opsin R/G, B), and retinal pigmented epithelium with RPE65 (green, RPE65, C), were used at 27-weeks of age to identify alterations in rod and cone outer segments. Scale bars= 50  $\mu$ m (A, B, and C). OS, outer segments; IS, inner segments; ONL, outer nuclear layer, INL, inner nuclear layer; RPE, retinal pigmented epithelium.

**2.5. Conditional *Sec10* fl/fl, *Best1-Cre*+ KO mice show significantly reduced rod visual function and RPE integrity as assessed by electroretinography (ERG).**

To correlate retinal structure with function, full field ERG responses were analyzed, capturing ERG *a*- and *b*-waves under dark-adapted scotopic conditions to determine rod photoreceptor function, as well as under photopic conditions after light adaptation to determine cone function. In addition, *c*-waves were determined after a prolonged light flash to assess RPE integrity. Visual function was assessed in Exoc5 fl/fl mice in the presence and absence of Best1-Cre at 6, 20 and 27 weeks of age. For ERGs with multiple light-intensities, a repeated measure ANOVA followed by a post hoc ANOVA with Bonferroni correction was performed, individual amplitudes were compared by T-test.

Within the wildtype/control group an amplitude by genotype interaction was identified for *b*- but not *a*-wave amplitudes (*a*-waves,  $p = 0.15$ ; *b*-waves,  $p < 0.02$ ), which was driven by larger *b*-wave amplitudes at 20 weeks of age. In the Exoc5 RPE KO (Exoc5fl/fl;Best1-Cre+) mice an amplitude by genotype interaction was also identified for *b*- but not *a*-wave amplitudes (*a*-waves,  $p = 0.33$ ; *b*-waves,  $p < 0.03$ ), which was driven by smaller *b*-wave amplitudes at 27 weeks of age ( $p = 0.003$ ). Cone amplitudes and *c*-wave amplitudes were unaffected by age in WT/control mice; whereas in Exoc5 RPE KO mice cone amplitudes remained stable but *c*-wave amplitudes dropped with age ( $p = 0.025$ ; 6 versus 27 weeks:  $p = 0.002$ ) (**Fig. 8 and Fig. S3**).

When the amplitudes were analyzed within the age groups, but differentiated by genotype, the following conclusions could be drawn. At 6 weeks of age, there was no difference in visual function and RPE integrity between the control and Exoc5 RPE KO mice (*a*-waves:  $p = 0.85$ , *b*-waves:  $p = 0.86$ , cones:  $p = 0.71$ , *c*-waves:  $p = 0.90$ ). At 20 weeks of age, a difference in rod visual function and RPE integrity between the control and sec10 RPE KO mice was identified (*a*-waves:  $p = 0.003$ , *b*-waves:  $p = 0.0001$ , cones:  $p = 0.45$ , *c*-waves:  $p = 0.024$ ). Likewise, at 27 weeks of age, a difference in rod visual function and RPE integrity between the control and Exoc5 RPE KO mice was identified (*a*-waves:  $p = 0.02$ , *b*-waves:  $p = 0.0006$ , cones:  $p = 0.41$ , *c*-waves:  $p = 0.020$ ) (**Fig. 8 and Fig. S3**).

In summary, eliminating Exoc5 from RPE impaired RPE *c*-wave amplitudes with age concomitant with a reduction in signals in the rod pathway whereas cone function was unaffected.

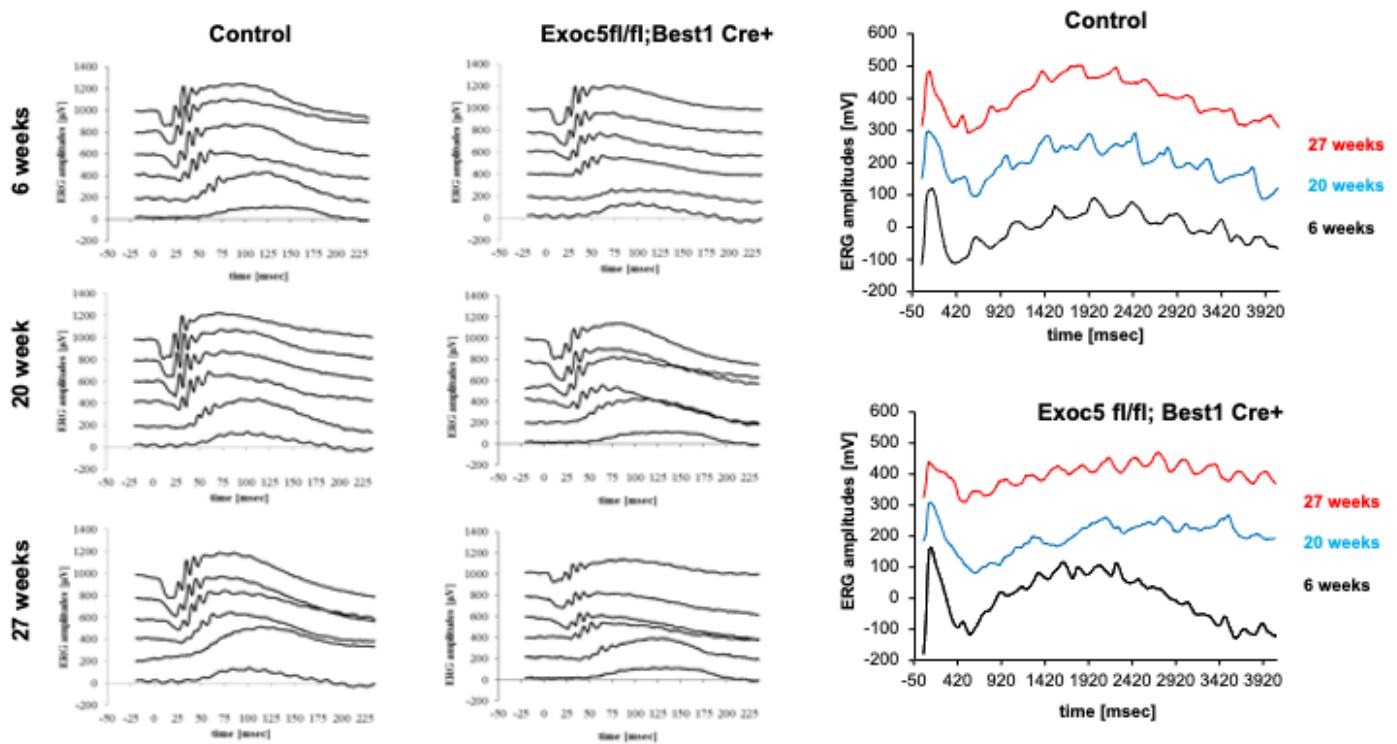


Fig. 8. Measurement of visual function in *Exoc5 fl/fl; Best1-Cre<sup>+</sup>* mice by full-field Electroretinography (ERG).

Dark-adapted, scotopic ERGs were recorded in response to increasing light intensities in cohorts of 6, 20, and 27-week old control (*Exoc5 fl/fl*) and *Exoc5 fl/fl; Best1-Cre<sup>+</sup>* mice. RPE-specific *Exoc5* knockout mice in which both copies of *Exoc5* were eliminated showed progressively significantly lower dark-adapted *a*- and *b*-wave amplitudes compared to controls (posthoc ANOVA: *a*-waves  $P < 0.03$ ; *b*-waves  $P < 0.01$ ), in particular at higher light intensities (20, 10, 6, 0 dB). Data are expressed as mean  $\pm$  SEM (*Exoc5 fl/fl; Best1-Cre<sup>+</sup>*:  $n=10$ ; and *Exoc5 fl/fl; Best1-Cre<sup>+</sup>* mice:  $n=10$ ).

### 3. Discussion

We report two principal findings here, both of which are of great interest. First, we show that the exocyst, which we previously showed is necessary for normal photoreceptor development and function [15], is also required for normal function and maintenance of the RPE. A strength of this paper is that we have dissected out RPE maintenance as the variable that we are studying. The RPE, and indeed the rest of the eye, was allowed to develop normally as cre expression in the *Best1-Cre* mouse first occurs only at ~P15 and is not maximal until P28 [17]. By examining 20 and 27-weeks eyes from Exoc5 RPE-specific KO mice, we show that the degeneration of the RPE is progressive and occurs after the conditional loss of Exoc5. In the eye, photoreceptor and RPE cells are ciliated. We have previously shown that the exocyst is necessary for ciliogenesis in the kidney [10], eye [15], ear [21], and heart [22]. Retinal degeneration is the most common phenotype among ciliopathy patients. Most research on the retinal phenotype has focused on retinal photoreceptors that contain a highly specialized primary cilium that is found to degenerate in ciliopathy animal models and patients. The contribution of other ciliated retinal cell types to retinal degeneration has not been investigated so far. The RPE is a ciliated monolayer epithelium that lies at the back of the eye and is essential for photoreceptor development and function. We hypothesize that loss of cilia function in the RPE cells is what is leading to loss of function of the RPE, which leads to progressive photoreceptor cell degeneration in our mouse model.

Second, and of equal importance, is that normal photoreceptor function seems to depend on normal RPE function. This is somewhat counterintuitive as the RPE is “downstream” of the photoreceptor in the visual process. So what might be the mechanism? It may be simply that the RPE can no longer clear extracellular vesicles (EVs) that are continuously shed from the photoreceptors, leading to a toxic effect in photoreceptors; however, there may be a more intriguing explanation. Two groups had shown that the primary cilia secrete small EVs (termed ectosomes) in *Chlamydomonas* [23] and *Caenorhabditis elegans* [24]. One group showed in mammalian cells, that, when activated, G protein-coupled receptors fail to undergo retrieval from cilia back into the cell. These G protein-coupled receptors concentrate into membranous buds at the tips of cilia before release into ectosomes, and hedgehog-dependent ectocytosis regulates ciliary signaling [25]. We recently showed in mammalian cells that not only do primary cilia secrete ectosomes, but that primary cilia are responsible for up to 60% of the small (50-150 nm) EVs that are secreted [26]. We hypothesize that there is crosstalk between the RPE and photoreceptors that is mediated by EVs going in both directions, and this hypothesis warrants further investigation.

Intracellularly, the exocyst localizes in other places besides the primary cilium, and the loss of Exoc5 driven by *Best1-Cre* likely causes ciliary defects in the RPE that lead to the retinal phenotypes. To further test this hypothesis, we are currently generating intraflagellar transport protein 88 (IFT88) fl/fl mice, which will be crossed with *Best-Cre* mice, to support the idea that primary cilia defects in RPE lead to the phenotype, including the photoreceptor defects, as *Ift88* is only expressed in primary cilia (it is a protein necessary to build primary cilia).

Taken together, our results not only provide insights into *exoc5* function and dysfunction but also suggest the existence of molecular network between *exoc5* function and the RPE/Photoreceptor crosstalk opening new perspective in utilizing this knowledge towards the development of novel therapeutic strategies for treatment of inherited retinal dystrophies.

## 4. Materials and Methods

### 4.1. Materials

All chemicals, unless stated otherwise, were purchased from Sigma-Aldrich (St. Louis, MO).

### 4.2. Animal use approval

All experiments on zebrafish and mice were approved by the Institutional Animal Care and Use Committee (IACUC) of the Medical University of South Carolina and the Ralph H. Johnson VAMC and were performed in compliance with the ARVO Statement for the Use of Animals in Ophthalmic and Vision Research.

### 4.3. Zebrafish Husbandry

Adult zebrafish were maintained and raised in an Aquatic Habitats recirculating water system (Tecniplast, West Chester, PA) in a 14:10-hour light-dark cycle and maintained under standard conditions at 28.5°C. The *exoc5* mutant zebrafish line was purchased from Zebrafish International Resource Center (ZIRC, Oregon, OR: *exoc5*-sa23168). This *exoc5* zebrafish mutant, contains a C>T point mutation at amino acid 377, resulting in a premature stop codon. The point mutation was verified by PCR and direct sequencing of both strands in both heterozygote adults and mutant larvae progeny. The transgenic *Tg(XIRho:EGFP)<sup>fl1</sup>*, WT (strain AB/TU) zebrafish lines has been described previously and was crossed with *exoc5*<sup>+/-</sup> animals to finally generate *exoc5*<sup>+/-</sup>;*Tg*-XOPS-GFP breeding pairs. The *Tg*:XOPS-GFP zebrafish line expresses soluble GFP driven by Rhodopsin in rod photoreceptor cells only (Fadool, 2003; Perkins and Fadool, 2010). Collected embryos were maintained in embryo medium (15 mM NaCl, 0.5 mM KCl, 1 mM CaCl<sub>2</sub>, 1 mM MgSO<sub>4</sub>, 0.15 mM KH<sub>2</sub>PO<sub>4</sub>, 0.05 mM NH<sub>2</sub>PO<sub>4</sub>, 0.7 mM NaHCO<sub>3</sub>) at 28.5 °C. Morphological features were used to determine the stage of the embryos in hours (hpf) or days (dpf) post fertilization. Genomic DNA from clipped fins, or whole 3.5 days post fertilized (dpf) zebrafish after phenotypes were observed, was extracted in 50 µL 1x lysis buffer (10 mM Tris-HCl pH 8.0, 50 mM KCl, 0.3% Tween 20, 0.3% NP40), denatured at 98 °C for 10 minutes, digested at 55 °C for 6 hours after 10 µg/mL proteinase K was added, and the reaction was stopped at 98 °C for 10 minutes. The PCR primers used for genotyping were, forward primer, 5'-CTA-TATAGACATGGAGCGGCAAT-3'; reverse primer: 5'- ccaacaattcctcacCTTCC-3'. Sequencing was performed by Genewiz with the forward primer used for PCR (Genewiz, South Plainfield, NJ).

### 4.4. Mouse Husbandry

Animals were kept in a 12-hour light-dark cycle with food and water *ad libitum*. The generation and genotyping of our *Exoc5*(Sec10) fl/fl mice has been described previously (16). The RPE-specific conditional *Exoc5* knockout mice were generated by crossing *Exoc5* fl/fl with Best1-Cre<sup>+</sup> mice (Jackson Laboratories, Bar Harbor, ME), and are designated as *Exoc5* fl/fl;Best1-Cre<sup>+</sup> in the manuscript (Fig. S1). *Exoc5* conditional mice were genotyped using the following set of PCR primers: forward primer, Fl-Exoc5 5'loxP#2F 5'-GCCTG-TAACTCACAGAGATC-3' with reverse primer, Fl-Exoc5 5'loxP#2R 5'-GCTGG-CATTCTAAGTCATGG-3', tDTomato: forward primer, 5'-CTCTGCTGCCTCCTGGCTTCTR-3' with reverse primer, 5'-TCAATGGGCGGGGTCGTT-3', Best1-Cre mice were identified using the following set of PCR primers: forward primer, 5' Cre-F:5'-TTGCCTGCATTACCGGTCGATGCAAC-GAGT-3'; reverse primer: Cre-R 5'-CCTGGTCGAAATCAGTGC GTTCGAACGCTA-3'.

#### 4.5. Mouse Retina Dissection, Immunohistochemistry and Fluorescence Imaging

Whole zebrafish or mouse eyes were enucleated and fixed by immersion in 4% paraformaldehyde in 1× phosphate buffer (PBS) for 2 hours at room temperature (RT). Eyes were incubated in a sucrose gradient of 5% sucrose in phosphate buffer (SPB) for 15 minutes at RT, 15% SPB for 15 minutes at RT, 30% SPB for 2 hours at RT, overnight in a 70:30 v/v ratio of OCT:SPB solution (Tissue-Tek, Sakura Finetech, Torrance, CA) at 4 °C. Eyes were then mounted in cyro-molds containing 70:30 v/v ratio of OCT:SPB solution and frozen on a dry-ice bath containing 100% ethanol. 12 μm thick sections were cut using a cryostat (Leica). Sections were air dried for 24 hours at RT and then subjected to immunohistochemistry. Blocking solution (1% BSA, 5% normal goat serum, 0.2% Triton-X-100, 0.1% Tween-20 in PBS) was applied for 2 hours in a humidified chamber. Primary antibodies were diluted in blocking solution as follows: ZPR3 (zebrafish eyes only; 1:100 dilution; ZIRC), 1D4 – Rhodopsin (for mouse eyes only; Sigma, St. Louis, MO), RPE65 (1:200 dilution; Sigma) and acetylated-α-tubulin (1:1000 dilution; Sigma, St. Louis, MO). Medium-wavelength cones were stained with R/G cone opsins (1:250 dilution, Molecular Probes, Eugene, OR). Conjugated PNA-488 antibody was purchased from Invitrogen Life Technologies (Carlsbad, CA) and used at 1:500 dilution, and 4',6-diamidino-2-phenylindole (DAPI; 1:10,000) was used to label nuclei. Sections were mounted in Vectashield (Vector Laboratories, Burlingame, CA). Z-stack images were collected using a Leica SP8 confocal microscope (Leica, Germany) and processed with the Leica Viewer software.

#### 4.6. Transmission Electron microscopy (TEM)

Control and *exoc5* mutant zebrafish larvae or WT and *Exoc5* fl/fl;Rho-Cre<sup>+</sup> mice eyes (or eyecups), were fixed in a solution containing 2.5% glutaraldehyde, 2% paraformaldehyde, and postfixed with 2% osmium tetroxide. The fixed tissue was sectioned to obtain radial sections at 1 μm and rinsed with cacodylate buffer (0.1 M), dehydrated through a graded ethanol series, and infiltrated with Epon resin. Samples were processed by the Electron Microscopy Resource Laboratory at the Medical University of South Carolina (MUSC) or the University of South Florida (USF) using a Joel Transmission Electron Microscope (JEM-1400Plus).

#### 4.7. Electroretinography (ERG)

Electroretinography (ERGs) recordings on mice were performed according to published procedures (18). Mice were dark-adapted overnight, anesthetized using xylazine (20 mg/kg) and ketamine (100 mg/kg), and pupils were dilated with 1 drop each of phenylephrine HCl (2.5%) and tropicamide (1%). Body temperature was stabilized via a DC-powered heating pad held at 37 °C. ERG recordings and data analyses were performed using the EPIC-4000 system (LKC Technologies, Inc.), using light stimuli with varying light intensities and wavelengths. Under scotopic conditions, responses to 10  $\mu$ s single-flashes of white light (maximum intensity of 2.48 photopic cd-s/m<sup>2</sup>) between 40 and 0 decibel (dB) of attenuation were measured. After light-adapting animals for 8 minutes with rod-saturating light [35], UV-cone responses were tested using LED flashes centered at 360 nm at a single light intensity. Peak a-wave amplitude was measured from baseline to the initial negative-going voltage, whereas peak b-wave amplitude was measured from the trough of the a-wave to the peak of the positive b-wave.

#### 4.8. Statistics

Results are presented as mean  $\pm$  standard deviation for image analysis, mean  $\pm$  standard error of the mean for electroretinography. For pairwise comparisons, statistical significance was assessed using the two-tailed Student's *t*-test. For ERG experiments, testing from the same animals over multiple light intensities, repeated measure ANOVA followed by Fisher's PLSD was used (StatView). For Western blot analysis, relative intensities of each band were quantified (densitometry) using ImageJ Software version 1.49 and normalized to the loading control.

**5. Conclusions:** Our results show the pathological consequences of condition *Exoc5* protein loss in RPE, on retinal cell function. Loss of *Exoc5* in RPE, resulted in progressive retinal cell degeneration and loss of visual function. Further studies using IFT88 mice are needed to confirm if loss of cilia results in these retinal phenotypes.

**Supplementary Materials:** The following are available online at [www.mdpi.com/xxx/s1](http://www.mdpi.com/xxx/s1), Supplementary Fig. S1: Generation of *tdTomatoExoc5fl/fl* mice and genotyping for conditional *tdTomatoExoc5fl/fl;Best1-Cre<sup>+</sup>* mice. Supplementary Fig. S2: Quantification of photoreceptor lengths. Supplementary Fig. S3: Measurement of visual function in *Exoc5fl/fl;Best1-Cre<sup>+</sup>* mice by full-field Electroretinography (ERG) and *c*-wave function.

**Author Contributions:** J.H.L., B.R., and G.P.L., designed the research studies and equally supervised this work. G.P.L and B.R., wrote the manuscript. G.P.L., E.O., S.W., Y.D., B.F., Y.S., M.R.B. and X.Z., conducted experiments and acquired data. J.H.L., G.P.L., A.A.K, M.R.B., and B.R., analyzed and interpreted the data. A.A.K and M.R.B., supplied reagents and edited the manuscript.

**Funding:** This work was supported in part by grants from the VA (Merit Award I01 BX000820 to J.H.L.; RX000444 and BX003050 to B.R.), NIH (P30DK074038 to J.H.L., R21EY025034 and R01EY030889 to G.P.L., and R01EY019320 to B.R.), American Heart Association AWRP Winter 2017 Collaborative Sciences Award (J. H. L.) and Dialysis Clinic, Inc (DCI) award to G.P.L. and J.H.L. NIH/NEI award EY027013-02 and USF Taneja College of Pharmacy startup grant to M.R.B.

**Conflicts of Interest:** "The funders had no role in the design of the study; in the collection, analyses, or interpretation of data; in the writing of the manuscript, or in the decision to publish the results". Author's declare no conflict of interest.

## References

1. Yorston D. Retinal Diseases and VISION 2020. *Community Eye Health*. 2003;16(46):19-20.
2. Gilbert C, and Foster A. Childhood blindness in the context of VISION 2020--the right to sight. *Bull World Health Organ*. 2001;79(3):227-32.
3. Wright AF, Chakarova CF, Abd El-Aziz MM, and Bhattacharya SS. Photoreceptor degeneration: genetic and mechanistic dissection of a complex trait. *Nat Rev Genet*. 2010;11(4):273-84.
4. Smyth BJ, Snyder RW, Balkovetz DF, and Lipschutz JH. Recent advances in the cell biology of polycystic kidney disease. *Int Rev Cytol*. 2003;231:51-89.
5. Webber WA, and Lee J. Fine structure of mammalian renal cilia. *Anat Rec*. 1975;182(3):339-43.
6. Choi SY, Chacon-Heszele MF, Huang L, McKenna S, Wilson FP, Zuo X, et al. Cdc42 deficiency causes ciliary abnormalities and cystic kidneys. *J Am Soc Nephrol*. 2013;24(9):1435-50.
7. Fogelgren B, Lin SY, Zuo X, Jaffe KM, Park KM, Reichert RJ, et al. The exocyst protein Sec10 interacts with Polycystin-2 and knockdown causes PKD-phenotypes. *PLoS Genet*. 2011;7(4):e1001361.
8. Seixas C, Choi SY, Polgar N, Umberger NL, East MP, Zuo X, et al. Arl13b and the exocyst interact synergistically in ciliogenesis. *Mol Biol Cell*. 2016;27(2):308-20.
9. Zuo X, Fogelgren B, and Lipschutz JH. The small GTPase Cdc42 is necessary for primary ciliogenesis in renal tubular epithelial cells. *J Biol Chem*. 2011;286(25):22469-77.
10. Zuo X, Guo W, and Lipschutz JH. The exocyst protein Sec10 is necessary for primary ciliogenesis and cystogenesis in vitro. *Mol Biol Cell*. 2009;20:2522-9.
11. Lipschutz JH, Guo W, O'Brien LE, Nguyen YH, Novick P, and Mostov KE. Exocyst is involved in cystogenesis and tubulogenesis and acts by modulating synthesis and delivery of basolateral plasma membrane and secretory proteins. *Mol Biol Cell*. 2000;11(12):4259-75.
12. Choi SY, Baek JI, Zuo X, Kim SH, Dunaief JL, and Lipschutz JH. Cdc42 and sec10 Are Required for Normal Retinal Development in Zebrafish. *Invest Ophthalmol Vis Sci*. 2015;56(5):3361-70.
13. Dixon-Salazar TJ, Silhavy JL, Udpa N, Schroth J, Bielas S, Schaffer AE, et al. Exome sequencing can improve diagnosis and alter patient management. *Sci Transl Med*. 2012;4(138):138ra78.
14. Khan AO, Oystreck DT, Seidahmed MZ, AlDrees A, Elmalik SA, Alorainy IA, et al. Ophthalmic features of Joubert syndrome. *Ophthalmology*. 2008;115(12):2286-9.
15. Lobo GP, Fulmer D, Guo L, Zuo X, Dang Y, Kim SH, et al. The exocyst is required for photoreceptor ciliogenesis and retinal development. *J Biol Chem*. 2017;292(36):14814-26.
16. Fogelgren B, Polgar N, Lui VH, Lee AJ, Tamashiro KK, Napoli JA, et al. Urothelial Defects from Targeted Inactivation of Exocyst Sec10 in Mice Cause Ureteropelvic Junction Obstructions. *PLoS One*. 2015;10(6):e0129346.
17. Iacovelli J, Zhao C, Wolkow N, Veldman P, Gollomp K, Ojha P, et al. Generation of Cre transgenic mice with postnatal RPE-specific ocular expression. *Invest Ophthalmol Vis Sci*. 2011;52(3):1378-83.
18. Woodell A, Coughlin B, Kunchithapautham K, Casey S, Williamson T, Ferrell WD, et al. Alternative complement pathway deficiency ameliorates chronic smoke-induced functional and morphological ocular injury. *PLoS One*. 2013;8(6):e67894.
19. Gargini C, Terzibasi E, Mazzoni F, and Strettoi E. Retinal organization in the retinal degeneration 10 (rd10) mutant mouse: a morphological and ERG study. *J Comp Neurol*. 2007;500(2):222-38.
20. Perkins BD, and Fadool JM. Photoreceptor structure and development analyses using GFP transgenes. *Methods Cell Biol*. 2010;100:205-18.

21. Lee B, Baek JI, Min H, Bae SH, Moon K, Kim MA, et al. Exocyst Complex Member EXOC5 Is Required for Survival of Hair Cells and Spiral Ganglion Neurons and Maintenance of Hearing. *Mol Neurobiol.* 2018;55(8):6518-32.
22. Fulmer D, Toomer K, Guo L, Moore K, Glover J, Moore R, et al. Defects in the Exocyst-Cilia Machinery Cause Bicuspid Aortic Valve Disease and Aortic Stenosis. *Circulation.* 2019;140(16):1331-41.
23. Wood CR, Huang K, Diener DR, and Rosenbaum JL. The cilium secretes bioactive ectosomes. *Curr Biol.* 2013;23(10):906-11.
24. Wang J, Silva M, Haas LA, Morsci NS, Nguyen KC, Hall DH, et al. *C. elegans* ciliated sensory neurons release extracellular vesicles that function in animal communication. *Curr Biol.* 2014;24(5):519-25.
25. Nager AR, Goldstein JS, Herranz-Perez V, Portran D, Ye F, Garcia-Verdugo JM, et al. An Actin Network Dispatches Ciliary GPCRs into Extracellular Vesicles to Modulate Signaling. *Cell.* 2017;168(1-2):252-63 e14.
26. Zuo X, Kwon SH, Janech MG, Dang Y, Lauzon SD, Fogelgren B, et al. Primary cilia and the exocyst are linked to urinary extracellular vesicle production and content. *J Biol Chem.* 2019;294(50):19099-110.